Ab Initio Calculations of the Anisotropic Dielectric Tensor of GaAs/AlAs Superlattices

Silvana Botti,[1,2] Nathalie Vast,[1] Lucia Reining,[1] Valerio Olevano,[1] and Lucio Claudio Andreani[2]

[1]*Laboratoire des Solides Irradiés, UMR 7642 CNRS-CEA, École Polytechnique, F-91128 Palaiseau, France*
[2]*INFM-Dipartimento di Fisica "A. Volta," Università di Pavia, Via Bassi 6, I-27100 Pavia, Italy*

The static dielectric properties of $(001)(GaAs)_p/(AlAs)_p$ superlattices have been calculated as a function of their period p for $1 \leq p \leq 12$, starting from density-functional theory. The interplay between quantum confinement and local field effects is shown to be crucial. For light polarized in the growth direction it leads to the otherwise surprising justification of the use of a classical effective medium theory, even for the smallest periods. Only the inclusion of both contributions allows in *ab initio* and in semiempirical calculations to reproduce the experimentally observed birefringence.

The electronic states of heterostructures differ from those of the constituent bulk materials, in particular due to the confinement at the nanoscale level, and to the reduction of symmetry, which can lead to a large optical anisotropy [1]. Nonlinear effects are responsible for the growing interest in superlattices (SL's) [2], especially GaAs based ones [3]. Both this nonlinearity and the optical anisotropy of GaAs/oxidized-AlAs SL's have been exploited to generate optical frequency conversion [4]. The GaAs/AlAs SL's are hence prototypes for the understanding of artificial structures, and their optical properties have been thoroughly investigated both experimentally [5] and theoretically [6] at frequencies close to the optical gap. However, very little information is available concerning their static dielectric properties. First, the refractive index n has not been measured, and it is commonly estimated from the dielectric constants of bulk GaAs and AlAs in the framework of the effective medium approach [7]. This classical theory is expected to fail for small period SL's, where quantum confinement is important. In fact, theoretical calculations have shown for ultrathin $(001)(GaAs)_p/(AlAs)_p$ SL's that the effective medium model cannot explain the behavior of the dielectric tensor for $p \leq 3$ [8]. However, the size limit at which the classical approach breaks down is not known. Second, the change in the refractive index with light polarization—the static birefringence Δn—has been measured for $(001)(GaAs)_p/(AlAs)_p$ SL's for $p \geq 6$, and a remarkably steep rise of the anisotropy with increasing p has been observed [9]. *Ab initio* methods for ultrathin SL's [8], and a semiempirical approach for larger ones [10], could not account for the observed value of the anisotropy nor for its behavior as a function of p, even *qualitatively*.

The birefringence in perturbed semiconductors has two contributions [11,12], namely, a dispersionless term involving high energy gaps between valence and conduction bands, and a resonant term associated with the gaps between the top valence and the first conduction bands. In SL's, the confinement potential induces a coupling of the folded GaAs and AlAs bulk states and a splitting at Γ of

the upper valence band. This symmetry-induced splitting into heavy-hole (hh) and light-hole (lh) subbands is of course an essential ingredient to explain the observed birefringence, since the hh and lh states couple differently to light polarization. However, if one assumes a simple one-by-one correspondence between the SL-perturbed transitions and, for example, the static birefringence, there are some important experimental observations which cannot be explained, in particular, the finite value of the static birefringence for large SL periods: since the relative contributions of the interfaces vanish for increasing p, also the anisotropy vanishes in the simplified picture of Fermi's golden rule for one-particle states, in which the macroscopic dielectric response is a sum of independent-particle transitions. Therefore, other features must play a crucial role, and important contributions to the SL response are expected from (i) the confinement effects on the gaps between occupied and empty states, (ii) the transition from a type-II to a type-I SL when the SL period increases [13], and (iii) in addition to the possibility of complicated many-body contributions, crystal local field effects (LFE) [9]. In view of the qualitative disagreement between experiment and existing calculations [8,10], a clear picture of the contribution of all these effects is crucial for an understanding of the SL dielectric response.

We have therefore calculated the two principal components of the static dielectric tensor, for light polarized in plane, $\varepsilon_\perp$, and along the SL growth direction, $\varepsilon_\parallel$, and the birefringence of $(001)(GaAs)_p/(AlAs)_p$ SLs for barrier/well periods $1 \leq p \leq 12$. We have performed *ab initio* calculations in the framework of the time-dependent density-functional theory (TDDFT) [14], which includes the LFE. The evolution of the dielectric tensor turns out to depend strongly on the interplay between quantum confinement and LFE. The anisotropy of the LFE is shown to be the essential ingredient in both *ab initio* and semiempirical calculations for the explanation of the experimentally observed behavior of the birefringence $\Delta n = \sqrt{\varepsilon_\perp} - \sqrt{\varepsilon_\parallel}$ as a function of p [9].

We first perform a ground-state calculation using DFT in the local density approximation (LDA), using norm-conserving pseudopotentials, a plane wave basis, and neglecting the spin-orbit splitting. From the Kohn-Sham wave functions ϕ_i, eigenvalues ϵ_i, and occupation numbers f_i, we construct the static independent-particle (RPA) polarizability χ^0:

$$\chi^0(\mathbf{r}, \mathbf{r}') = 2 \sum_{i,j} (f_i - f_j) \frac{\phi_i(\mathbf{r})\phi_j^*(\mathbf{r})\phi_i^*(\mathbf{r}')\phi_j(\mathbf{r}')}{\epsilon_i - \epsilon_j}. \quad (1)$$

The RPA microscopic dielectric function is related to χ^0 by $\varepsilon = 1 - v\chi^0$. The macroscopic dielectric tensor ε_M measured in optical experiments, contains the contributions of both macroscopic and microscopic variations of the potentials as a response to the applied macroscopic field. These can be either calculated explicitly, as done in density-functional perturbation theory [15], or, as we do in the present work, expressed in the reciprocal lattice (**G**) space:

$$\varepsilon_M = \lim_{\mathbf{q} \to 0} \frac{1}{\varepsilon_{\mathbf{G}=\mathbf{G}'=0}^{-1}(\mathbf{q})} = \lim_{\mathbf{q} \to 0} \left\{ \varepsilon_{\mathbf{00}}(\mathbf{q}) - \sum_{\mathbf{G},\mathbf{G}' \neq 0} \varepsilon_{0,\mathbf{G}}(\mathbf{q}) (\varepsilon_{\mathbf{G}_1,\mathbf{G}_2 \neq 0})_{\mathbf{G}\mathbf{G}'}^{-1} \varepsilon_{\mathbf{G}',0}(\mathbf{q}) \right\}. \quad (2)$$

For an applied ($\mathbf{G}' = 0$) field, microscopic ($\mathbf{G}, \mathbf{G}' \neq 0$) variations of the response contribute to ε_M through the matrix inversion, to be precise, through the off-diagonal elements of ε: these transition-mixing contributions [the last term of Eq. (2)] are the LFE [16].

The upper panel of Fig. 1 shows the components of the dielectric tensor as a function of the SL period p, calculated in RPA and neglecting LFE. First, ε is essentially increasing with increasing p, since the gaps between occupied and empty states decrease due to a decrease of confinement. Second, for large SL periods, ε tends to the average of the bulk dielectric constants of GaAs and AlAs calculated without LFE (arrow in Fig. 1). This occurs for both polarizations, so that the birefringence tends to zero, consistently with the fact that the weight of
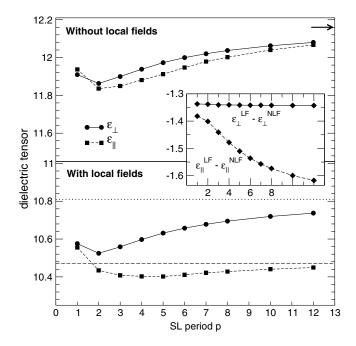
the contributions of the interfaces relative to the weight of bulk states vanishes for increasing p. Third, $\varepsilon_\perp$ is always closer to the average value than $\varepsilon_\parallel$ for $p > 2$, as on average the gap is smaller for light polarized in plane rather than in the growth direction. In other words, the confinement is rather "seen" in growth than in the in-plane direction, making the birefringence slightly positive at those p. The lower panel of Fig. 1 shows the same quantities calculated including LFE. As usual, LFE decrease the absolute value of the dielectric tensor components. The decrease of ε is found to be more effective for $\varepsilon_\parallel$ than for $\varepsilon_\perp$, showing that the wing elements $\varepsilon_{\mathbf{0},\mathbf{G}}$ and $\varepsilon_{\mathbf{G},\mathbf{0}}$ are particularly sensitive to the presence of the interfaces (the body $\varepsilon_{\mathbf{G}_1,\mathbf{G}_2 \neq 0}$ does not contain the $\mathbf{q}$ dependence if $\mathbf{q} \to 0$) [17]. In the growth direction, when the SL period increases, the increasingly negative contribution of the LFE cancels the rise of the first term in Eq. (2) containing the independent-particle transitions (see the inset in Fig. 1). Therefore, $\varepsilon_\parallel$ is always close to the effective medium value estimated with the theoretical bulk constants calculated including LFE, $\varepsilon_\parallel^{-1} = (\varepsilon_{GaAs}^{-1} + \varepsilon_{AlAs}^{-1})/2$ (dashed line). Contrastingly, in the in-plane direction, the direct effect of the confinement on the independent transitions is found to be larger than its effect on the LFE. The latter are found to be almost constant with the period (see the inset of Fig. 1), and the slope of the linear behavior of $\varepsilon_\perp$ remains therefore unchanged. Consequently, the effective medium value $\varepsilon_\perp = (\varepsilon_{GaAs} + \varepsilon_{AlAs})/2$ (dotted line) is reached only very slowly at an extrapolated period $p \simeq 20$.

The anisotropy of the LFE has now important consequences on the calculated birefringence reported in Fig. 2 as a function of the well width, together with the experimental results (circles). Without LFE (empty squares) one obtains an anisotropy much smaller than in experiment and vanishing in the limit of large SL periods, thus confirming the results of Ref. [10]: the measured anisotropy does not come directly from an anisotropy of the independent transitions [18]. The inclusion of the LFE (filled squares) drastically changes the behavior of the birefringence, whose amplitude increases now up to

FIG. 1. Dielectric tensor calculated without (ε^{NLF}, upper panel) and with (ε^{LF}, lower panel) LFE and their difference (inset), as a function of the SL period p. Arrow: average of bulk GaAs and AlAs dielectric constants, calculated without LFE. Dotted (dashed) line: effective medium value of $\varepsilon_\perp$ ($\varepsilon_\parallel$).

the effective medium value $\Delta n \simeq 0.05$ estimated from the RPA ε_{GaAs} and ε_{AlAs} (shaded region representing our numerical convergence error on the RPA plateau value). Therefore LFE are sufficient to qualitatively explain the experimentally observed birefringence.

To understand more in detail the origin of the LFE in terms of mixing of transitions, we consider "all" the conduction bands, i.e., those necessary to achieve convergence, as possible final states for the transitions in Eq. (1), but we restrict the initial states to the v first valence bands, for the SL period $p = 3$ and $p = 8$ (Fig. 3). Note that in order to scale the results, the abscissa axis is shown as $v = ip$, i being an integer. The behavior of the birefringence for all the SL periods is similar to the two examples presented here: the lowest bands do not contribute, and when the LFE are neglected, the large positive contribution arising from bands $4p$ to $6p$ is almost completely canceled by the bands between $7p$ and $8p$. Also in the LFE (difference between circles and squares in Fig. 3) the contributions of the bands cancel and even change the sign of these effects; their contribution is dominated by the bands $7p$ to $8p$ and finally becomes positive. A similar analysis of the contributions of the conduction bands shows that the birefringence is dominated by the anisotropy of the LFE involving transitions to the lowest conduction bands. The cancellation effects are important, in fact, a calculation involving only the highest valence and lowest conduction bands yields a
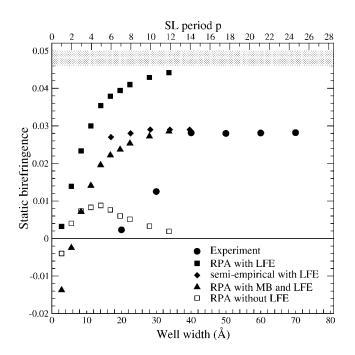
contribution of LFE which is overestimated by about a factor of 10. The observed anisotropy can hence not be explained in a simple model including few transitions.

The calculated plateau in Fig. 2 has a higher value than the experimental one. This is a consequence of the well-known error of the local density and RPA approximations on the dielectric constants of bulk materials [15]. To go beyond the RPA, we have checked the inclusion of exchange-correlation effects within the adiabatic local density approximation (TDLDA) [19]. These effects are known to significantly change the dielectric constants of bulk semiconductors: consistently with earlier results [16,20], we find that the TDLDA bulk dielectric constants of both constituent materials increase by as much as 7% with respect to the RPA ones. However, the changes completely cancel out in the birefringence, and both the plateau value and the slope with which it is reached remain unchanged. A direct inclusion in *ab initio* calculations of further many-body effects is today out of reach. We have therefore used the fact that the Slater-Koster contact interaction model [21] describes well the excitonic effects in simple semiconductors. Generalizing this model for the case of an anisotropic material, it turns out that the full dielectric constants $\varepsilon_{\parallel}$ and $\varepsilon_{\perp}$ are approximately proportional to their RPA counterparts $\varepsilon_{\parallel}^{RPA}$ and $\varepsilon_{\perp}^{RPA}$, with factors $\alpha_{\parallel}$ and $\alpha_{\perp}$ which are essentially independent of p. $\alpha_{\parallel}$ and $\alpha_{\perp}$ can be fitted using, in the plateau region, the calculated and the measured ε. The static birefringence can then be obtained for all p's, as shown by the triangles in Fig. 2: the quantitative agreement with experiment is now greatly improved. It should, however, again be stressed that only the inclusion of LFE allows one to obtain the correct *qualitative* behavior of the birefringence and the classical limit.

Finally, one might wonder about the influence of details of the band structure, as the nature of the gap (the transition from a type-II to a type-I SL occurs earlier in the *ab initio* calculation than in experiments). This
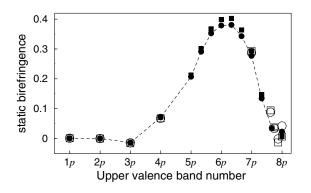

FIG. 2. Static birefringence for $(GaAs)_p/(AlAs)_p$ SL's as a function of p. Circles: experiment from Ref. [9]. Empty (filled) squares: RPA calculations without (with) LFE. Triangles: RPA calculations including LFE and modeled many-body (MB) effects. Diamonds: semiempirical approach with LFE. Shaded region: RPA effective medium value.

FIG. 3. Contribution to the birefringence of the valence bands for $p = 3$ (filled symbols) and $p = 8$ (empty symbols). Circles: contributions with LFE; squares: contributions without LFE. The dashed line is a guide to the eyes for the $p = 3$ SL with LFE.

feature, as well as the width of the gap and the bulk dielectric constants are instead correctly reproduced, by construction, in the semiempirical approach used in Ref. [10], which, in the Fermi's golden rule framework, had not been able to explain the increasing birefringence. We have therefore used in Eq. (1) the semiempirical electronic band structure for medium to large SL periods. Including now LFE (diamonds in Fig. 2), the results perfectly agree with the experiment for the value of the plateau. This is important, since it shows that the semiempirical approach works very well at large SL periods, if the dominant contributions (here the LFE) are included. Instead, in the semiempirical approach the plateau is reached too early, since the semiempirical potentials do not give enough flexibility to the interface electronic states. For a more detailed comparison and before including further many-body effects in the *ab initio* calculations, it would be worthwhile to perform birefringence measurements such as those in Ref. [9] on smaller period SL's with well characterized interfaces, and, in particular, to extend the experiment to lower temperatures.

In conclusion, we have calculated the dielectric properties of $(001)(GaAs)_p/(AlAs)_p$ SL's as a function of the period and compared them to the results of the effective medium theory: the use of the latter is found to be justified in the growth direction even for small periods. In the in-plane direction, however, quantum confinement effects are dominant. Local field effects are responsible for the observed overall behavior of the anisotropy, while further many-body effects lead only to quantitative corrections. The classical limit of the birefringence is reached for a period of $p \approx 12$: any (semiempirical or *ab initio*) approach determining the macroscopic dielectric tensor must hence include local field effects beyond Fermi's golden rule and one-electron transitions in order to explain the well-width dependence of the macroscopic dielectric tensor and its anisotropy. The same effects are found within the *ab initio* (both RPA and TDLDA) and the semiempirical approaches.

[1] See, e.g., D. Kovalev *et al.*, Appl. Phys. Lett. **78**, 916 (2001).

[2] Y. Y. Zhu and N. B. Ming, Opt. Quantum Electron. **31**, 1093 (1999).

[3] D. C. Hutchings and B. S. Wherrett, Phys. Rev. B **52**, 8150 (1995); K. J. Luo *et al.*, Appl. Phys. Lett. **70**, 2825 (1997).

[4] A. Fiore *et al.*, Nature (London) **391**, 463 (1998).

[5] M. Garriga *et al.*, Phys. Rev. B **36**, 3254 (1987); O. Günther *et al.*, *ibid.* **52**, 2599 (1995); U. Schmid *et al.*, *ibid.* **45**, 3546 (1992).

[6] K. B. Kahen and J. P. Leburton, Phys. Rev. B **33**, 5465 (1986); J. B. Xia and Y. C. Chang, *ibid.* **42**, 1781 (1990); R. G. Dandrea and A. Zunger, *ibid.* **43**, 8962 (1991); E. Ghahramani, D. J. Moss, and J. E. Sipe, *ibid.* **43**, 9269 (1991); E. Herbert Li, J. Appl. Phys. **82**, 6251 (1997); Y. E. Kitaev *et al.*, J. Phys. Condens. Matter **9**, 257 (1997); S. S. Li and B. F. Zhu, *ibid.* **10**, 6311 (1998).

[7] D. J. Bergman, Phys. Rep. **43**, 391 (1978); M. G. Cottam and D. R. Tilley, in *Introduction to Surface and Superlattice Excitations* (Cambridge University Press, Cambridge, 1989), p. 267; E. Jahne, Phys. Status Solidi (b) **194**, 279 (1996).

[8] M. Alouani *et al.*, Phys. Rev. Lett. **61**, 1643 (1988).

[9] A. A. Sirenko *et al.*, Phys. Rev. B **60**, 8253 (1999).

[10] S. Botti and L. C. Andreani, Phys. Rev. B **63**, 235313 (2001).

[11] M. Cardona, in *Atomic Structure and Properties of Solids*, edited by E. Burstein (Academic Press, New York, 1972), p. 514.

[12] P. Etchegoin *et al.*, Phys. Rev. B **53**, 13 662 (1996).

[13] A. Franceschetti and A. Zunger, Phys. Rev. B **52**, 14 664 (1995); H. Fu and A. Zunger, Phys. Rev. Lett. **80**, 5397 (1998); M. Hosoda *et al.*, Phys. Rev. B **56**, 6432 (1997).

[14] E. Runge and E. K. U. Gross, Phys. Rev. Lett. **52**, 997 (1984).

[15] S. Baroni, P. Giannozzi, and A. Testa, Phys. Rev. Lett. **58**, 1861 (1987); P. Giannozzi *et al.*, Phys. Rev. B **43**, 7231 (1991).

[16] See, e.g., S. Baroni and R. Resta, Phys. Rev. B **33**, 7017 (1986), and references therein.

[17] A detailed discussion will be given in S. Botti *et al.* (unpublished).

[18] This is similar to what has been found in the naturally anisotropic material TiO_2: see N. Vast *et al.*, Phys. Rev. Lett. **88**, 037601 (2002).

[19] E. K. U. Gross and W. Kohn, Phys. Rev. Lett. **55**, 2850 (1985); **57**, 923 (1986).

[20] M. S. Hybertsen and S. G. Louie, Phys. Rev. B **35**, 5585 (1987).

[21] R. M. Martin *et al.*, Phys. Rev. B **6**, 2500 (1972); J. E. Rowe and D. E. Aspnes, Phys. Rev. Lett. **25**, 162 (1970).

[22] S. Baroni *et al.*, http://www.pwscf.org.